HHS Public Access

Author manuscript

Neuron. Author manuscript; available in PMC 2015 August 13.

Published in final edited form as:

Neuron. 2013 April 10; 78(1): 191–204. doi:10.1016/j.neuron.2013.02.007.

Circuits for grasping: spinal dI3 interneurons mediate cutaneous control of motor behavior

Tuan V. Bui[2], **Turgay Akay**[3,4], **Osama Loubani**[2], **Thomas S. Hnasko**[5], **Thomas M. Jessell**[3], and **Robert M. Brownstone**[1,2]

[1]Department of Surgery (Neurosurgery), Dalhousie University, Halifax, Nova Scotia, Canada B3H 4R2

[2]Department of Medical Neuroscience, Dalhousie University, Halifax, Nova Scotia, Canada B3H 4R2

[3]Howard Hughes Medical Institute, Kavli Institute for Brain Science, Departments of Neuroscience, and Biochemistry and Molecular Biophysics, Columbia University, New York, NY 10032, USA

[4]Department of Neurological Surgery, Center for Motor Neuron Biology and Disease, Columbia University, New York, NY 10032, USA

[5]Department of Neurosciences, University of California San Diego, La Jolla CA 92093, USA

SUMMARY

Accurate motor performance depends on the integration in spinal microcircuits of sensory feedback information. Hand grasp is a skilled motor behavior known to require cutaneous sensory feedback, but spinal microcircuits that process and relay this feedback to the motor system have not been defined. We sought to define classes of spinal interneurons involved in the cutaneous control of hand grasp in mice, and show that dI3 interneurons, a class of dorsal spinal interneurons marked by expression of Isl1, convey input from low threshold cutaneous afferents to motoneurons. Mice in which the output of dI3 interneurons has been inactivated exhibit deficits in motor tasks that rely on cutaneous afferent input. Most strikingly, the ability to maintain grip strength in response to increasing load is lost following genetic silencing of dI3 interneuron output. Thus, spinal microcircuits that integrate cutaneous feedback crucial for paw grip rely on the intermediary role of dI3 interneurons.

INTRODUCTION

Coordinated movement relies on the integration of sensory feedback signals with core motor circuits. In mammals, motor performance is refined by sensory feedback signals that convey

Correspondence: Rob Brownstone, Departments of Surgery (Neurosurgery) and Medical Neuroscience, Dalhousie University, P.O. Box 15000, Halifax, NS, Canada B3H 4R2, phone: +1-902-494-6244, fax: +1-902-494-1212, Rob.Brownstone@dal.ca.

information from proprioceptive afferents as well as from mechanoreceptive afferents activated by diverse cutaneous receptors. This information is integrated in spinal motor circuits to ensure that intended movements conform to environmental context. Defining spinal microcircuits involved in the integration of sensory inputs represents one approach to obtaining insight into the physiological control of motor actions.

Studies of sensory integration in spinal motor microcircuits have largely focused on the influence of proprioceptive inputs on spinal neurons in the cat (Jankowska, 2008; McCrea, 2001). In recent years, the use of molecular genetic techniques has yielded insight into the integration of proprioceptive afferent activity in motor circuits in mice (Mentis et al., 2006; Pecho-Vrieseling et al., 2009; Sürmeli et al., 2011; Tripodi et al., 2011;Wang et al., 2008). Cutaneous afferents also regulate the output of spinal motor circuits, notably in the control of locomotion (Burke et al., 2001; Drew and Rossignol, 1987; Duysens and Pearson, 1976; Forssberg, 1979; Quevedo et al., 2005). But the identity and circuitry of spinal interneurons that process and transmit cutaneous afferent signals to motoneurons remain largely unknown.

Studies of interneurons comprising spinal circuits have typically relied on locomotor activity as the assay of motor circuit function (Brownstone and Bui, 2010; Fetcho and McLean, 2010; Grillner and Jessell, 2009). Many of the core features of locomotor activity can be produced by “central pattern generators” – the fundamental rhythm and pattern of walking can be obtained without sensory feedback. In contrast, motor activities such as object manipulation and hand grip appear to be more dependent on cutaneous sensory input (Witney et al., 2004).

Emerging evidence indicates that sensory feedback from cutaneous mechanoreceptors regulates the force and precision of grasp tasks (Witney et al., 2004). Moreover, spinal interneurons active during grip have been recorded in the macaque monkey (Fetz et al., 2002; Takei and Seki, 2010), but it remains unclear whether the activity of these interneurons is influenced by sensory feedback, and whether these neurons actually play a critical role in the spinal circuits for grip control. Short-latency cutaneous-evoked reflexes to motoneurons have been identified in the cat (Egger and Wall, 1971; Hongo et al., 1989a,b; Moschovakis et al., 1992), supporting the existence of excitatory interneurons involved in the integration of cutaneous sensation. But the involvement of such interneurons in motor behavior is not known.

In this study, we aimed to define and manipulate, through their distinguishing molecular character, sets of spinal interneurons with roles in mediating cutaneous control of motor output relevant to grasping. We reasoned that spinal interneurons that control grip would be located in deep dorsal/intermediate laminae, the site of termination of cutaneous afferents (Brown et al., 1981; Todd, 2010). We focused on a class of neurons called dI3 interneurons (dI3 INs) (Ericson et al., 1992; Gross et al., 2002; Müller et al., 2002). dI3 INs represent one of six classes of “early-born” dorsally-derived interneurons, and can be distinguished from other spinal interneurons by their expression of the LIM homeodomain transcription factor Isl1 (Helms and Johnson, 2003; Liem et al., 1997). We show that dI3 INs form excitatory glutamatergic synapses with motoneurons and in turn receive low threshold cutaneous

afferent input. Eliminating glutamatergic transmission from these interneurons results in a profound loss of grip strength. dI3 INs are therefore an interneuron class necessary for spinal interneuronal microcircuits crucial for cutaneous regulation of paw grasp.

RESULTS

dI3 INS are located in intermediate laminae

The location of yellow fluorescent protein $(YFP)^+$ dI3 INs and choline acetyltransferase $(ChAT)^+$ motoneurons was determined in P13-P20 *Isl1*$^{+/Cre}$; *Thy1*-lox-stop-lox-YFP ("*Isl1*-YFP") spinal cord. YFP$^+$/ChAT^{null} dI3 INs (Figure 1Ai-iii) were present along the length of the spinal cord, and were detected in roughly equal proportions in laminae V, VI, and VII in lumbar (Figure 1B-E) and cervical (Figure S1) spinal cord, in regions where cutaneous afferents from the limbs are known to terminate (Todd, 2010).

dI3 INS are Glutamatergic Premotor Interneurons

We determined the transmitter phenotype of dI3 INs by assessing the expression of the vesicular glutamate transporter vGluT2 in Isl1-YFP$^+$ INs in P13-P20 mice. We found that ~85% of dI3 INs expressed vGluT2 (Figure 2A). The presence of vGluT2^{null}/YFP$^+$ autonomic motoneurons in rostral sections combined with the imperfect sensitivity of this technique may have led to an underestimate of the true proportion of glutamatergic dI3 INs. None of the Isl1-YFP$^+$ boutons expressed GlyT2, GAD65, or GAD67 (data not shown), indicating that dI3 INs are neither glycinergic nor GABAergic. Together, these data indicate that the vast majority, and probably all dI3 INs, possess glutamatergic transmitter phenotypes.

We determined whether dI3 INs form direct connections with spinal motoneurons by examining spinal cords from *Isl1*$^{+/Cre}$;*Thy1*-loxP-stop-loxP-mGFP mice, in which Cre-directed membrane-bound green fluorescent protein (GFP) labels a small proportion (< 1%) of Isl1-expressing neurons and their axons. We detected GFP$^+$ axons which formed bouton-like varicosities along motoneuron dendrites (Figure 2B). Furthermore, following intracellular injections in dI3 INs in *Isl1*-YFP mice, neurobiotin-labeled axons with bouton-like structures were detected in apposition to the dendrites of YFP$^+$ motoneurons (Figures 2C-2D), often seen as clusters of boutons (Figure 2D, dashed boxes). We also detected vGluT2$^+$/YFP$^+$ boutons in apposition to the somata and the proximal 100 μm of in-plane dendrites of ChAT$^+$ motoneurons (10.0 ± 5.3, n = 140 boutons on 14 motoneurons; Figure 2E; Figure S2A for cervical motoneuron). To explore whether vGluT2$^+$/YFP$^+$ boutons originated from supraspinal YFP$^+$ neurons, the spinal cords of *Isl1*-YFP mice (n = 2) were transected at the thoracic level and the animals examined 7 days later. The density of vGluT2$^+$/YFP$^+$ boutons on motoneuronal somata and proximal 100 μm of in-plane dendrites (6.6 ± 4.1, n = 93 boutons on 14 motoneurons) was similar to that found in non-spinalized mice ($p = 0.07$; Figure 2F), excluding that YFP$^+$ boutons contacting motoneurons derive primarily from supraspinal neurons. Rabies virus trans-synaptic tracing has also identified dI3 INs as a source of synaptic input to motoneurons (Stepien et al., 2010). Thus glutamatergic dI3 INs project directly to motoneuron somata and dendrites (Figure 2G).

vGluT2$^+$/YFP$^+$ boutons were also detected in intermediate laminae of cervical and lumbar segments (12.8 ± 4.1 boutons/1000 μm^3, n = 5 sections from 2 spinal cords, Figure S2B). Some of these boutons were in apposition to other dI3 INs (Figure S2C). Thus both motoneurons and INs are targets of dI3 INs.

dI3 INS Receive Monosynaptic Sensory Input

We determined whether dI3 INs receive direct input from primary sensory afferents. Expression of vGluT1 marks low threshold cutaneous and proprioceptive primary afferent fibers and is excluded from spinal interneurons (Alvarez et al., 2004; Oliveira et al., 2003; Todd et al., 2003). We used vGluT1 as a molecular marker of direct afferent input to dI3 INs (Figure 3A). We found that 88% of YFP$^+$ dI3 INs (n = 46 out of 52 neurons) were contacted by vGluT1$^+$ boutons (9.2 ± 3.7 boutons/dI3 IN soma and proximal dendrites, n = 18). In early postnatal spinal cord, parvalbumin (PV) serves as a marker of proprioceptive afferents (Mentis et al., 2006). Both vGluT1$^+$/PV$^+$ (n = 26) and vGluT1$^+$/PV^{null} boutons (n = 85) were detected on dI3 INs at P1-P7 (n = 21, 1-4 optical sections per neuron were analyzed) (Figure 3B). Thus, proprioceptive and cutaneous sensory afferents converge on dI3 INs. Analysis of labeling of vGluT1 in adult spinal cord tissue examined 7 days after thoracic spinalization (n = 2) revealed no diminution in the number of vGluT1$^+$ boutons apposed to dI3 INs (n = 18 dI3 INs, 11.9 ± 8.0 boutons /dI3 IN, p = 0.2; Figure 3C), consistent with the view that these boutons derive from sensory afferents.

We used whole-cell patch-clamp recordings to assess physiological connectivity between sensory afferents and dI3 INs. All dI3 INs in P5-P16 *Isl1*-YFP mice (n = 51, input resistance: 626 ± 356 MΩ) discharged repetitively. However, ~1/6 did not fire until after a delay of > 50 ms due to expression of a 4-AP-sensitive slowly inactivating potassium (I_D-type) current (Figure 4A and Figure S3). Thus transient synaptic excitation could elicit spike firing in most (~5/6) dI3 INs.

We then assessed sensory input using electrical stimulation of L4 or L5 dorsal roots, and revealed that 105 out of 114 (92%) dI3 INs had sensory-evoked excitatory responses (Figure 4B). Of these 105 dI3 INs, 31 (30%) responded with a single EPSP or action potential, and 35 (33%) with a pattern comprised of an early EPSP or action potential followed by a longer lasting IPSP (Figure 4Bi). The remaining 39 (37%) neurons responded with a sustained membrane depolarization that conferred repetitive firing in response to brief dorsal root (DR) stimulation (Figure 4Bii). Voltage-clamp recordings of responses to DR stimulation demonstrated CNQX-sensitive, multiphasic EPSCs of up to several hundred pAs (Figure 4C-D, n = 5), with reversal potentials near 0 mV (Figure 4E, n = 3). Thus dI3 INs receive strong glutamatergic inputs from primary sensory afferents, in some cases mixed with longer latency excitatory and/or inhibitory inputs.

We measured the latency and jitter (Vrieseling and Arber, 2006) of dorsal root-evoked EPSCs (drEPSCs) to determine whether early responses were monosynaptic. The onset latencies of drEPSCs in dI3 INs from P5-P16 *Isl1*-YFP mice ranged from 2.0 ms to 20.0 ms. Latencies of known monosynaptic responses – ventral root reflexes and low threshold sensory-evoked EPSCs in motoneurons – were in the order of 2.0 – 2.5 ms (Figures 4Fi). drEPSC latencies below 3 ms were considered monosynaptic and were detected in 51 of 105

dI3 INs and (Figure 4Fi, 4Gi). Both low and high jitter responses were seen (Figure 4Fii-iii). A variance below 0.01 ms^2 was taken as indicative of monosynaptic input (Doyle and Andresen, 2001). Responses in 36 of 105 dI3 INs met this criterion (Figure 4Gii). Based upon these stringent criteria for latency and jitter, 32 of 105 (30%) dI3 INs received clear monosynaptic sensory input. The mean drEPSC latencies and jitters decreased with postnatal age (Figure 4Giii, see Jennings and Fitzgerald, 1998; Mears and Frank, 1997), suggesting that this is an underestimate of what would be found in mature mice. Thus dI3 INs receive monosynaptic input from sensory afferents.

To probe the class of sensory afferents that synapse on dI3 INs, we next stimulated DRs with increasing stimulus intensities. While in the adult cat, stimulation of different afferent types can be controlled by the strength of stimulation, similar thresholds have not been established in young mice. Nevertheless, fibers will be recruited in order based upon their diameters and states of myelination (Erlanger and Gasser, 1930). Due to ongoing myelination and changes in thresholds and conduction velocities during earlier postnatal stages (Lizarraga et al., 2007), we restricted this analysis to recordings of dI3 INs between P12 and P16 (Figure 4H). Stimulation intensities were graded and are reported as factors of threshold (T) for evoking a monosynaptic ventral root reflex. Regardless of latency or jitter of response, every dI3 IN responded to low threshold stimulation (n = 19). A quarter of these dI3 INs (n = 5 of 19) responded solely to low threshold stimulation, whereas the remaining 3/4 also responded to medium and/or high threshold stimuli (Figure 4Hiii). These findings parallel the different molecular labeling of primary afferent boutons apposing dI3 INs (above, Figure 3C), and support the view that dI3 INs integrate a number of sensory modalities, including proprioceptive and low-threshold cutaneous afferents. Taken together with the evidence that dI3 INs project directly to motoneurons, these data suggest that dI3 INs are involved in low threshold disynaptic reflex pathways (Figure 4I).

dI3 INS mediate disynaptic cutaneous-evoked reflexes

To examine the function of dI3 INs, we used genetic techniques to eliminate glutamate output from their terminals, by crossing *Isl1*$^{+/Cre}$ mice to vGluT2$^{flox/flox}$ mice (dI3^{OFF} mice; Figure 5A). To confirm an effective reduction in glutamatergic capacity, we asked: (a) if vGluT2 mRNA expression is reduced or eliminated in dI3 INs; (b) if vGluT2 protein is eliminated from the boutons of dI3 INs in apposition to MNs; (c) if low threshold primary afferent input to dI3 INs is unaffected; and (d) if sensory receptors or motoneurons are affected.

In dI3^{OFF} mice, traces of vGluT2 mRNA were detected in only 28% of dI3 INs (n = 91 of 330 neurons in 2 mice, P13-P20; Figure 5B). Secondly, YFP$^+$ dI3 INs still projected to motoneurons (Figure 5C), but there was a 93% reduction in vGluT2$^+$/YFP$^+$ boutons in apposition to ChAT$^+$ motoneuronal somata and proximal 100 μm of dendrites in plane (0.7 boutons/motoneuron, n = 10 motoneurons, P13-P20; Figure 5D). Thirdly, primary afferent inputs to dI3 INs were unaffected in dI3^{OFF} mice, as demonstrated both immunohistochemically (8 out of 9 dI3 INs, 8.8 ± 7.3 vGluT1$^+$/YFP$^+$ boutons per dI3 IN, P13-P20; Figure 5E) and electrophysiologically (drEPSCs were seen in 8 out of 10 dI3 INs from P13-P14 dI3^{OFF} mice, similar to the frequency seen in *Isl1*-YFP mice, chi-square, p =

0.2; in 4 of these 8 dI3 INs, these EPSCs met strict short–latency, low jitter thresholds, similar to the 5 out of 8 cells seen in *Isl1*-YFP at similar age range, chi-square, $p = 0.6$; Figure 5F). Moreover, normal sensory-evoked monosynaptic reflexes were recorded from ventral roots (Figure 5F), suggesting that vGluT1 function was not altered in primary afferents. Fourthly, expression of vGluT2 in Merkel cells, cutaneous transduction cells that express Isl1 and mediate low threshold mechanical input from the paws (Haeberle et al., 2004; Maricich et al., 2009), was unaffected in $dI3^{OFF}$ mice (Figure S4A). In addition there were no changes in mechanical nociception as assessed by von Frey hair testing in these mutant mice (Figure S4C). Finally, no motoneuronal dysfunction was found: there was no apparent weakness during treadmill walking (data not shown), and no alterations in motor responses (M-waves) or monosynaptic (H-) reflexes (see below). Together, these data suggest that the primary consequence of the genetic manipulation used to make $dI3^{OFF}$ mice is not dysfunction of the afferent system, but is rather the loss of glutamatergic output of dI3 INs.

To assess whether there was cutaneous afferent input to dI3 INs, we first labeled afferents of the sural nerve and detected boutons in apposition to dI3 INs (Figure 6A, $n = 3$). We then used sural nerve stimulation in neonatal and adult preparations in $dI3^{OFF}$ and control mice to assess this putative disynaptic pathway. Stimulation of the sural nerve in in vitro preparations (P1-P3, Figure 6C) led to L5 DR volleys of longer delay (1–2.5 ms, $n = 5$, Figure 6D) than those obtained with tibial nerve stimulation, consistent with slower conduction velocities in cutaneous compared to muscle afferents. The thresholds for eliciting these responses were similar for the two nerves, (2 – 4 μA), demonstrating that although we cannot be specific about the fiber type stimulated, we were using the lowest possible currents to evoke responses.

We next assessed disynaptic reflex responses. The latencies of ventral root reflexes in response to sural nerve stimulation were 4-5 ms ($n = 3$) longer than their latencies in response to tibial nerve stimulation (Figure 6E), reflective of the fact that tibial nerve stimulation elicits monosynaptic Ia afferent-evoked reflexes and suggesting that the reflex evoked by sural nerve stimulation involves one to two additional synapses (Figure 6B). The stimulation thresholds for eliciting short-latency reflexes by sural nerve stimulation ranged between 1.5–2 T ($n = 5$), where T is defined as the smallest stimulation strength at which a DR volley was seen. This suggests that the short-latency response from sural nerve stimulation is mediated by cutaneous afferents, possibly of low threshold.

In $dI3^{OFF}$ mice, DR volleys in response to sural nerve stimulation were similar to those in control mice (Figure S5A), but the mean normalized short-latency ventral root response was significantly smaller ($p < 0.05$, Figure 6F) in $dI3^{OFF}$ mice (1.1 ± 0.3, mean ± pooled SD, $n = 4$) compared to control mice (3.2 ± 0.8, $n = 7$). The short-latency reflexes were present in 6 of 7 control animals as opposed to 0 of 4 $dI3^{OFF}$ animals ($p < 0.05$, chi-square), indicating that dI3 INs mediate a short-latency, likely disynaptic cutaneous to motor reflex in neonatal mice.

To determine whether dI3 INs mediate this reflex in awake adult mice (Figure 6G), we first ensured that monosynaptic reflexes are not affected in $dI3^{OFF}$ mice. Single pulse tibial nerve

stimulation (Figure 6Hi) produced both a direct motor response (M-wave) and a monosynaptic reflex response (H-reflex, latency in the range of 2-3 ms, Figure 6Hii). Both the M-wave and H-reflex were observable in control and in dI3^{OFF} animals, and the ratios of H-reflex to M-wave, calculated at 2T, were similar ($p = 0.2$) in controls (0.19 ± 0.06, $n = 3$) and mutants (0.30 ± 0.16, $n = 4$), indicative of normal Ia afferent reflexes and motoneuron activity in dI3^{OFF} mice.

To test short-latency reflexes evoked by sural nerve stimulation, we ensured that we were not stimulating high threshold sural nerve afferents by adjusting stimulation strengths to be in the range at which short-latency responses were first seen in cord dorsum potential (CDP) recordings ($n = 1$ control and 2 dI3^{OFF} animals; Figures 6H and S5B); these stimuli were below nociceptive thresholds as determined by vocalizations. Sural nerve stimulation did not produce short-latency responses in tibialis anterior (TA) in either control or mutant mice. However, a short-latency reflex was present in gastrocnemius (Gs) in 8 of 11 control mice as compared to only 2 of 8 dI3^{OFF} mice (chi-square, $p < 0.05$), despite using multiple shocks to potentiate the response (Figure 6Ii). The mean normalized EMG response was 1.8 ± 1.4 (mean ± pooled SD) in dI3^{OFF} mice ($n = 8$) compared to 4.1 ± 3.5 in control littermates ($n = 11$, $p < 0.05$, Figure 6Iii). This loss or reduction of motor response to sural nerve stimulation in dI3^{OFF} mice indicates that dI3 INs mediate a short-latency low threshold cutaneous-motor reflex (Figure 6J).

dI3 INS are Necessary for Normal Grip Function

To assess how silencing the output of the dI3 INs affects motor tasks that require cutaneous afferent feedback, we first tested the performance of mutants with a locomotor task. On a horizontal ladder with uniform spacing between rungs, the number of hindlimb missteps was greater in dI3^{OFF} mice (control: 2.8 ± 3.0 slips per 100 steps; dI3^{OFF}: 9.2 ± 5.7 slips per 100 steps; $p < 0.05$, Figure 7A). In addition, falls from the ladder were occasionally observed during testing of dI3^{OFF} mice but never with control littermates. This suggests that the hindlimbs rely on dI3 INs to ensure appropriate grip of the ladder rungs during ladder walking.

To explore further the functional consequence of eliminating dI3 IN output, we turned to a paw grip task that involves low threshold cutaneous receptors (Witney et al., 2004). Both control and dI3^{OFF} adult mice attempted to grasp the metal bars (indicating they could sense the bars), but the volar surfaces (forelimb and hindlimb) of the paws of dI3^{OFF} mice did not fully grip the bars (Figure 7B). During slow inversion of the cage top, the dI3^{OFF} mice would often slide down the grid due to an apparent failure to maintain adequate grip strength (Movie S1). The angle at which the dI3^{OFF} mice were unable to remain on the cage top was $58 \pm 12°$ from the horizontal axis (mean ± pooled SD; $n = 3$ trials for 3 mice; Figure 7C). When the grid was inverted to angles beyond vertical, dI3^{OFF} mice were unable to hang onto the grid ($n = 10$ out of 10, 3 trials each; 7 males, 3 females; between P30 – P120; Figure 7D and Movie S1). Control littermates could hang on for long periods averaging 50 s per trial ($n = 12$ out of 12, 3 trials each; 4 males, 8 females; between P30–P120; Figure 7D and Movie S2). These data suggest that the silencing of the output of dI3 INs impairs grasping and the ability to regulate grip strength in the face of an increasing load.

To determine whether the loss of grip function resulted from dysfunction within the spinal cord, we studied the forepaw grasp reflex in neonatal animals at an age prior to maturation of descending systems (Amendola et al., 2004; Fox, 1965). While 35 of 36 control pups (P1-P7) had reflexive palmar flexion in response to gentle stroking of the palmar surface, a stimulus that would activate low threshold mechanoreceptors, only 2 of 11 $dI3^{OFF}$ mutant pups exhibited this grasp reflex (Figure 7E, chi-square, $p < 0.05$). Taken together, these behavioral experiments provide evidence that spinal microcircuits involving dI3 INs mediate disynaptic reflex pathways from low threshold cutaneous afferents to motoneurons (Figure 7F) and play key roles in motor behaviors that involve cutaneous afferent feedback, notably the regulation of forelimb and hindlimb grip strength.

DISCUSSION

The spinal cord contains the neural circuitry necessary to produce a wide range of motor behaviors. However, the roles of particular neurons and their microcircuits in the execution of motor behaviors are poorly understood. We have identified a class of spinal interneurons, dI3 INs, that participate in a microcircuit necessary for cutaneous regulation of motor output. We show that dI3 INs mediate a disynaptic cutaneous-motor reflex circuit, and that this microcircuit is critical for the normal regulation of grasping in response to a changing environment. Thus dI3 INs form spinal microcircuits necessary for this specific motor behavior.

dI3 INs are involved in a disynaptic cutaneous-motor microcircuit

Studies of sensory-motor control in primates, including humans, have largely focused on the role of cutaneous inputs in forelimb, in particular hand, function (Witney et al., 2004). Insights from these studies have revealed that hand function is reliant on cutaneous input. But the spinal circuits involved in cutaneous-motor control of hand function have not been defined. We used knowledge of the molecular development of the mouse spinal cord that has been useful for genetic characterization of spinal locomotor circuits (Grossmann et al., 2010; Kiehn, 2011) to address microcircuits involved in the sensorimotor integration necessary for hand function.

The loss of a cutaneous-motor reflex in $dI3^{OFF}$ mice resulted from the functional loss of the internuncial neurons in the pathway, dI3 INs, through deletion of vGluT2. The reflex or behavioral deficits observed in $dI3^{OFF}$ mice would not have resulted from deletion of vGluT2 from primary afferents, as in the spinal cord, large diameter primary afferents originating from proprioceptors and low threshold mechanoreceptors express vGluT1, whereas vGluT2 is confined to small diameter afferents from high threshold nociceptors (Alvarez et al., 2004; Brumovsky et al., 2007; Landry et al., 2004). Furthermore, we demonstrate that in $dI3^{OFF}$ mice, low threshold afferent input to dI3 INs is not affected, whereas cutaneous short latency reflex pathways are disrupted. Although we detected traces of vGluT2 mRNA in about one-quarter of dI3 INs in the $dI3^{OFF}$ mice, 93% of dI3 axon boutons in motor pools were devoid of vGluT2 protein, indicating that this was an effective strategy to reduce neurotransmission from dI3 INs. Together, this indicates that the deficit in the reflex pathway was the elimination of vGluT2 in dI3 INs and hence the output from dI3

INs to motoneurons. In sum, the preservation of input to dI3 INs, the loss of vGluT2 in dI3 IN boutons in motor pools, together with the loss of reflex responses in short-latency time windows in dI3^{OFF} mice suggests that the same interneurons that receive cutaneous inputs project to motoneurons, forming a disynaptic cutaneous sensory-motor microcircuit.

dI3 INs as mediators of grip control

Elimination of vGluT2 from dI3 INs leads to the loss of a specific motor behavior – grasp – with minimal deficits in other motor tasks studied. That is, although the deficit seen in the ladder task in dI3^{OFF} mice suggests that dI3 INs integrate cutaneous input necessary for appropriate hindlimb placement, the most profound deficit was the inability of dI3^{OFF} mice to regulate grip control. Whether loss of grip function is due solely to loss of functional output from dI3 INs to motoneurons and/or to interneurons in intermediate laminae remains unclear. Nevertheless, it is likely that dI3 INs are involved in mediating haptic input necessary for many behaviors, and that our assay – grip testing – reveals one clear deficit.

Like the loss of cutaneous-motor reflexes, the behavioral deficits in dI3^{OFF} mice result from a functional deficit in dI3 INs. The behavior cannot be explained by disruption of cutaneous Merkel cells, as elimination of these sensory receptors does not lead to any deficit in the wire hang test (Maricich et al., 2012). Corresponding to this, deletion of vGluT2 from various dorsal root ganglion neurons led to a reduction in thermal and/or mechanical nociception (Lagerström et al., 2010; Scherrer et al., 2010), and a deficit in the response to intense but not light mechanical stimulation (Liu et al., 2010). Deletion of vGluT2 from all sensory neurons (Lagerström et al., 2010; Pietri et al., 2003) did not result in any motor deficits as assessed by rotarod or balance beam (Rogoz et al., 2012), or wire hang testing (Klas Kullander, personal communication). Together, this indicates that the deficits observed were not related to deficits in the afferent system.

The involvement of dI3 INs in grasp circuitry is consistent with their role in mediating sensory information from cutaneous mechanosensitive receptors, which mediate their effects via low threshold afferents. This afferent system plays a key role in mediating grip in humans (Dimitriou and Edin, 2008; Johansson and Flanagan, 2009). Humans cannot perform gripping tasks accurately following local anaesthetization of the fingers or hand (Augurelle et al., 2003; Johansson and Westling, 1984). As in dI3^{OFF} mice, this deficit could not be compensated by feed-forward descending control, i.e. the required grip and load forces could not accurately be predicted (Monzee et al., 2003; Witney et al., 2004), and maximal attainable pinch force was reduced (Augurelle et al., 2003). Our findings indicate that in mice the cutaneous input necessary to regulate grip strength is processed in a spinal microcircuit involving dI3 INs.

Previous studies have examined supraspinal mechanisms involved in primate hand function (Baker, 2011; Fuglevand, 2011; Schieber, 2011), but the spinal circuits that mediate this goal-directed motor behavior are not understood. Grip types can be broadly divided into two categories: precision grip and power grip (Napier, 1956; Young, 2003). Recent studies have demonstrated that propriospinal neurons in C3/C4 segments are critical for executing a reach-and-precision grip task in primates (Alstermark et al., 2011; Kinoshita et al., 2012), but the microcircuits regulating power grip, which require cutaneous feedback control so

that grip can be adjusted to unexpected environmental cues (Witney et al., 2004), have not been previously defined. The spinal neurons that are responsible for regulating grip strength would be ideal candidates to mediate the integration of feedback and feed-forward commands to appropriately regulate grip strength. We have shown that dI3 INs process feedback signal, and suggest that they may also integrate descending commands for grip.

Evolutionary and human considerations

The development of the hand and foot and the concurrent development of their neural control circuits were key adaptations in evolution. Prior to the evolution of precision grip and fine finger movements, basic hand function – in particular the power grip – provided significant evolutionary advantages. The ability of lizards to grip fine tree branches, and rapidly release and re-grip allowed them to navigate narrow branches (Abdala et al., 2009). These rather simple yet important grip functions predated the evolution of more complex grips in humans (Young, 2003), and would have required the development or exaptation of appropriate spinal control circuits. One candidate population from which dI3 INs could have developed are *Xenopus* tadpole dorsolateral ascending (dla) interneurons, as these are also glutamatergic, receive cutaneous inputs, and project to other spinal neurons (Li et al., 2004). In addition, non-human primate studies have demonstrated activity of spinal interneurons in a location similar to that of dI3 INs during grasp, suggesting that they may be responsible for combining and coordinating multiple hand muscles during precision grip tasks (Takei and Seki, 2010). Interneurons in this intermediate region that are tuned to grip strength receive inputs from cutaneous afferents (Fetz et al., 2002) and multiple descending systems (Riddle and Baker, 2010). The similar locations and inputs of these interneurons in the mouse, cat, and monkey suggest that dI3 INs, which play a critical role in paw function, are conserved features of mammalian spinal cord organization.

We have described a spinal microcircuit in mice that underlies a disynaptic grasp reflex. The normal grasp reflex evoked by palmar cutaneous stimulation in the neonate is absent in the $dI3^{OFF}$ mice. Similarly, activity of an orthologous spinal microcircuit may be responsible for the grasp reflex in the human infant. Human foetuses develop a grasp reflex in the first trimester (Hooker, 1938) that persists in the post-natal period for 2-6 months (Halverson, 1937; Pollack, 1960). Reflexive grasping is not normally seen in adult humans, likely because higher systems regulate this microcircuit, which may also be involved in feed-forward control of hand function (see Rushworth and Denny-Brown, 1959). Presumably, these reflexes disappear because of development of the brain and descending systems. Grasp reflexes emerge in adults with structural brain (Walshe and Hunt, 1936) and neurodegenerative diseases and their pathological reemergence can be quite disabling for both hand (Mestre and Lang, 2010) and foot function (Paulson and Gottlieb, 1968). In addition, the opposite effect – loss of normal control of hand grasp such as seen after spinal cord injury – is significantly disabling (Anderson, 2004). Understanding dI3 INs and their control will aid in the development of microcircuit-targeted therapies to improve hand dysfunction in disease or following injury.

Methods

Animals

Expression of YFP driven by the promoter for the homeodomain transcription factor Isl1 was obtained in double transgenic offspring of *Isl1*$^{+/Cre}$ and *Thy1*.lox-stop-lox.YFP mice.

The following strains of mice were generously donated and used in this study: *Thy1*.lox-stop-lox.YFP mice (from J. Sanes), and *Thy1*.lox-stop-lox.mGFP (from S. Arber). Conditional knockout of vGluT2 in Isl1 expressing neurons (dI3^{OFF}) was accomplished by crossing *Isl1*$^{+/Cre}$ mice with a strain of mice bearing a conditional allele of the *Slc17a6* (vGluT2) gene where exon 2 of the gene was flanked by *lox* sequences (vGluT2$^{flox/flox}$; Figure 5A). This results in Cre-mediated excision of exon 2 of the vGluT2 gene in Isl1 expressing neurons (Hnasko et al., 2010). All animal procedures were approved by the University Committee on Laboratory Animals of Dalhousie University and conform to the guidelines put forth by the Canadian Council for Animal Care. Additional methodological details can be found in Supplemental Information.

Electrophysiology

In-vitro spinal cord preparations—Sagittal hemicords were prepared from *Isl1*-YFP or from dI3^{OFF} postnatal (P5-P16) mice. Following anaesthesia administered by an injection of a mixture of xylazine and ketamine, mice were decapitated and spinal cords isolated by vertebrectomy in room temperature recording ACSF (in mM: NaCl, 127; KCl, 3; NaH_2PO_4, 1.2; $MgCl_2$, 1; $CaCl_2$, 2; $NaHCO_3$, 26; D-glucose, 10). Ventral and dorsal roots were dissected as distally as possible. Cords were hemisected by a midline longitudinal incision, were incubated for 45-60 minutes in 37° C recording ACSF, and then equilibrated in room temperature recording ACSF for at least 30 minutes. Hemicords were then pinned, medial-side up to a base of clear Sylgard (Dow Corning) and perfused with room temperature recording ACSF. Ventral and dorsal root activity was recorded via suction electrodes (A-M Systems Inc., Carlsborg, WA). Fluorescent dI3 INs were targeted based on their location in the intermediate spinal cord, taking care to not record from cells that were deep (motoneurons). Most recordings were from L4 and L5 segments, but if recording in rostral lumbar segments, neurons near the surface (possible autonomic motoneurons) were also avoided.

Electrophysiological testing of sensory inputs—Sensory fibers have different recruitment thresholds depending on the size of the fiber and the degree of myelination (Erlanger and Gasser, 1930). To express stimulation strength, we defined threshold (T) as either the lowest stimulus strength at which DR volleys or CDPs were first seen (if electrodes present), or at which ventral root responses were seen. We classified the responses of dI3 INs into low threshold (1-2 T), which would include group I muscle afferents and low threshold cutaneous afferents (Aβ) but may also include some group II and Aδ fibers, and high threshold (5-10 T), which putatively includes group III-IV muscle afferents and unmyelinated C-fiber nociceptive afferents. Intermediate stimuli were classified as medium threshold. T was typically between 4 and 20 μA in vitro.

In vivo measurement of EMG response to nerve stimulation—Adult mice were implanted with bipolar EMG recording electrodes (Pearson et al., 2005; Akay et al., 2006) as well as cuff electrodes to stimulate the tibial and/or sural nerves. Following 1-3 weeks of recovery, nerves were stimulated using single or pairs of 250 μs pulses for the tibial nerve, or using trains of 2 to 5 pulses for the sural nerve, at frequencies of 500 Hz, with an interval of 2 seconds between trains. Stimulation strengths used to attempt to elicit reflexes ranged between 75 and 500 μA (mean: 307 ± 135 μA, n = 11) in the control animals, and 40 to 750 μA (mean: 248 ± 228 μA, n = 8) in the mutant animals ($p = 0.31$). In contrast, the nociceptive threshold (producing vocalizations) ranged between 300 μA and 1500 μA (mean: 821 ± 356 μA, n = 7) in the control animals, and between 250 μA and 900 μA (mean: 571 ± 216 μA, n = 7) in the mutant animals ($p = 0.07$). The differences between the stimulation used to elicit the short-latency reflexes and the threshold for vocalization were significant (paired t test, $p < 0.05$, n = 5 control and 2 $dI3^{OFF}$ animals). In 4 animals we implanted chronic epidural cord dorsum electrodes to determine stimulation thresholds (n = 2 mutant and 2 controls). The threshold to elicit short-latency cord dorsum responses from sural nerve stimulation was between 100 and 300 μA (Figure S5B; n = 2 mutants and a control), i.e. in the same range we used to elicit reflex responses.

Reflex quantification

To quantify putative disynaptic responses in vitro, recordings were rectified and integrated in a time window from 14-22 ms after the onset of the DR volley (Figure 6B), and expressed as a ratio of the pre-stimulus integrated voltage.

In vivo, EMG responses were similarly quantified in a 4-8 ms window following the last stimulus (Figure 6B).

Behavioral Analysis

Wire hang test—To test grip strength, adult mice were placed on a cage top. The cage top was shaken to encourage gripping of the horizontal bars. The cage top was slowly inverted and positioned at least thirty centimeters above the landing surface. The latency to fall was measured. Each mouse underwent this test three times in a single day. In some mice, we repeated the test three times on a separate day. The results did not vary in the additional trials. The average weight of the $dI3^{OFF}$ mice (16.0 ± 3.7 g, n = 5) was not significantly greater than that of the control littermates (16.0 ± 2.6 g, n = 7).

Forepaw grasp reflex—To test for the presence of a forepaw grasp reflex in neonates (P1-P7), we gently stroked the palmar surface of the forepaw and observed any flexion of the fingers. This test was performed without prior knowledge of the genotype of the pups.

Additional behavioral analyses are described in Supplemental Information.

Statistical analysis

Unless otherwise noted, data are reported as mean ± SD and comparisons were performed using Student’s unpaired t-test with unequal variance with the threshold for significance set at 0.05.

Supplementary Material

Refer to Web version on PubMed Central for supplementary material.

ACKNOWLEDGMENTS

We thank Angelita Alcos, Bithika Ray, Apiraami Thana and Nadia Farbstein for excellent technical assistance; Joshua Sanes, and Silvia Arber for the generous contribution of mouse strains; Natalie Parks and Dan Marsh for help with the chronic spinalization; Jason Meissner and Allison Reid for aid with the von Frey test; Anatoliy Voskresenskiy and Leigh Sadler for work with the horizontal ladder experiments; Jonathan Carp and Jonathan Wolpaw for their suggestions in designing the nerve cuff electrodes; Jacob Schreckengost, Patrick Whelan, and Meggie Reardon for help with the isolated spinal cord preparation with sural nerve in continuity; Frédéric Bretzner, Pratip Mitra, Philippe Magown, Izabela Panek and Sabrina Tazerart for discussions, and Kevin Bourke for photography. T.V.B. was supported by a Nova Scotia Health Research Foundation fellowship and a CIHR Fellowship. T.M.J. is an Investigator of the Howard Hughes Medical Institute, and was supported by NIH R01-NS033245, Project A.L.S., and the Harold and Leila Mathers Foundation. This research was undertaken, in part, thanks to funding to R.M.B. from the Canada Research Chairs program. This work was funded by the Canadian Institutes of Health Research (FRN 79413).

REFERENCES

Abdala V, Manzano AS, Tulli MJ, Herrel A. The tendinous patterns in the palmar surface of the lizard manus: functional consequences for grasping ability. Anat. Rec. (Hoboken). 2009; 292:842–853. [PubMed: 19462454]

Akay T, Acharya HJ, Fouad K, Pearson KG. Behavioral and electromyographic characterization of mice lacking EphA4 receptors. J. Neurophysiol. 2006; 96:642–651. [PubMed: 16641385]

Alstermark B, Pettersson LG, Nishimura Y, Yoshino-Saito K, Tsuboi F, Takahashi M, Isa T. Motor command for precision grip in the macaque monkey can be mediated by spinal interneurons. J. Neurophysiol. 2011; 106:122–126. [PubMed: 21511706]

Alvarez FJ, Villalba RM, Zerda R, Schneider SP. Vesicular glutamate transporters in the spinal cord, with special reference to sensory primary afferent synapses. J. Comp. Neurol. 2004; 472:257–280. [PubMed: 15065123]

Amendola J, Verrier B, Roubertoux P, Durand J. Altered sensorimotor development in a transgenic mouse model of amyotrophic lateral sclerosis. Eur. J. Neurosci. 2004; 20:2822–2826. [PubMed: 15548226]

Anderson KD. Targeting recovery: priorities of the spinal cord-injured population. J. Neurotrauma. 2004; 21:1371–1383. [PubMed: 15672628]

Augurelle AS, Smith AM, Lejeune T, Thonnard JL. Importance of cutaneous feedback in maintaining a secure grip during manipulation of hand-held objects. J. Neurophysiol. 2003; 89:665–671. [PubMed: 12574444]

Baker SN. The primate reticulospinal tract, hand function and functional recovery. J. Physiol. 2011; 589:5603–5612. [PubMed: 21878519]

Brown AG, Fyffe RE, Rose PK, Snow PJ. Spinal cord collaterals from axons of type II slowly adapting units in the cat. J. Physiol. 1981; 316:469–480. [PubMed: 7320876]

Brownstone RM, Bui TV. Spinal interneurons providing input to the final common path during locomotion. Prog. Brain Res. 2010; 187:81–95. [PubMed: 21111202]

Brumovsky P, Watanabe M, Hökfelt T. Expression of the vesicular glutamate transporters-1 and -2 in adult mouse dorsal root ganglia and spinal cord and their regulation by nerve injury. Neuroscience. 2007; 147:469–490. [PubMed: 17577523]

Burke RE, Degtyarenko AM, Simon ES. Patterns of locomotor drive to motoneurons and last-order interneurons: clues to the structure of the CPG. J.Neurophysiol. 2001; 86:447–462. [PubMed: 11431524]

Dimitriou M, Edin BB. Discharges in human muscle receptor afferents during block grasping. J. Neurosci. 2008; 28:12632–12642. [PubMed: 19036957]

Doyle MW, Andresen MC. Reliability of monosynaptic sensory transmission in brain stem neurons in vitro. J. Neurophysiol. 2001; 85:2213–2223. [PubMed: 11353036]

Drew T, Rossignol S. A kinematic and electromyographic study of cutaneous reflexes evoked from the forelimb of unrestrained walking cats. J. Neurophysiol. 1987; 57:1160–1184. [PubMed: 3585458]

Duysens J, Pearson KG. The role of cutaneous afferents from the distal hindlimb in the regulation of the step cycle of thalamic cats. Exp. Brain Res. 1976; 24:245–255. [PubMed: 1253857]

Egger MD, Wall PD. The plantar cushion reflex circuit: an oligosynaptic cutaneous reflex. J. Physiol. 1971; 216:483–501. [PubMed: 5559630]

Ericson J, Thor S, Edlund T, Jessell TM, Yamada T. Early stages of motor neuron differentiation revealed by expression of homeobox gene Islet-1. Science. 1992; 256:1555–1560. [PubMed: 1350865]

Erlanger J, Gasser HS. The action potential in fibers of slow conduction in spinal roots and somatic nerves. Am. J. of Physiol. 1930; 92:43–82.

Fetcho JR, McLean DL. Some principles of organization of spinal neurons underlying locomotion in zebrafish and their implications. Ann. NY Acad. Sci. 2010; 1198:94–104. [PubMed: 20536924]

Fetz EE, Perlmutter SI, Prut Y, Seki K, Votaw S. Roles of primate spinal interneurons in preparation and execution of voluntary hand movement. Brain Res. Brain Res. Rev. 2002; 40:53–65. [PubMed: 12589906]

Forssberg H. Stumbling corrective reaction: a phase-dependent compensatory reaction during locomotion. J.Neurophysiol. 1979; 42:936–953. [PubMed: 479924]

Fox WM. Reflex-ontogeny and behavioural development of the mouse. Anim. Behav. 1965; 13:234–241. [PubMed: 5835840]

Fuglevand AJ. Mechanical properties and neural control of human hand motor units. J. Physiol. 2011; 589:5595–5602. [PubMed: 22005677]

Grillner S, Jessell TM. Measured motion: searching for simplicity in spinal locomotor networks. Curr. Opin. Neurobiol. 2009; 19:572–586. [PubMed: 19896834]

Gross MK, Dottori M, Goulding M. Lbx1 specifies somatosensory association interneurons in the dorsal spinal cord. Neuron. 2002; 34:535–549. [PubMed: 12062038]

Grossmann KS, Giraudin A, Britz O, Zhang J, Goulding M. Genetic dissection of rhythmic motor networks in mice. Prog. Brain Res. 2010; 187:19–37. [PubMed: 21111198]

Haeberle H, Fujiwara M, Chuang J, Medina MM, Panditrao MV, Bechstedt S, Howard J, Lumpkin EA. Molecular profiling reveals synaptic release machinery in Merkel cells. Proc. Natl. Acad. Sci. USA. 2004; 101:14503–14508. [PubMed: 15448211]

Halverson H. Studies of the grasping responses of early infancy. J. Genet. Psychol. 1937; 51:371–449.

Helms AW, Johnson JE. Specification of dorsal spinal cord interneurons. Curr. Opin. Neurobiol. 2003; 13:42–49. [PubMed: 12593981]

Hnasko TS, Chuhma N, Zhang H, Goh GY, Sulzer D, Palmiter RD, Rayport S, Edwards RH. Vesicular glutamate transport promotes dopamine storage and glutamate corelease in vivo. Neuron. 2010; 65:643–656. [PubMed: 20223200]

Hongo T, Kitazawa S, Ohki Y, Sasaki M, Xi MC. A physiological and morphological study of premotor interneurones in the cutaneous reflex pathways in cats. Brain Res. 1989; 505:163–166. [PubMed: 2611672]

Hongo T, Kitazawa S, Ohki Y, Xi MC. Functional identification of last-order interneurons of skin reflex pathways in the cat forelimb segments. Brain Res. 1989; 505:167–170. [PubMed: 2611673]

Hooker D. The origin of the grasping movement in man. Proc. Am. Phil. Soc. 1938; 79:587–606.

Jankowska E. Spinal interneuronal networks in the cat: elementary components. Brain Res. Rev. 2008; 57:46–55. [PubMed: 17884173]

Jennings E, Fitzgerald M. Postnatal changes in responses of rat dorsal horn cells to afferent stimulation: a fibre-induced sensitization. J. Physiol. 1998; 509(Pt 3):859–868. [PubMed: 9596805]

Johansson RS, Flanagan JR. Coding and use of tactile signals from the fingertips in object manipulation tasks. Nat. Rev. Neurosci. 2009; 10:345–359. [PubMed: 19352402]

Johansson RS, Westling G. Roles of glabrous skin receptors and sensorimotor memory in automatic control of precision grip when lifting rougher or more slippery objects. Exp. Brain Res. 1984; 56:550–564. [PubMed: 6499981]

Kiehn O. Development and functional organization of spinal locomotor circuits. Curr.Opin.Neurobiol. 2011; 21:100–109. [PubMed: 20889331]

Kinoshita M, Matsui R, Kato S, Hasegawa T, Kasahara H, Isa K, Watakabe A, Yamamori T, Nishimura Y, Alstermark B, et al. Genetic dissection of the circuit for hand dexterity in primates. Nature. 2012; 487:235–238. [PubMed: 22722837]

Lagerström MC, Rogoz K, Abrahamsen B, Persson E, Reinius B, Nordenankar K, Olund C, Smith C, Mendez JA, Chen ZF, et al. VGLUT2-dependent sensory neurons in the TRPV1 population regulate pain and itch. Neuron. 2010; 68:529–542. [PubMed: 21040852]

Landry M, Bouali-Benazzouz R, El Mestikawy S, Ravassard P, Nagy F. Expression of vesicular glutamate transporters in rat lumbar spinal cord, with a note on dorsal root ganglia. J. Comp. Neurol. 2004; 468:380–394. [PubMed: 14681932]

Li WC, Soffe SR, Roberts A. Dorsal spinal interneurons forming a primitive, cutaneous sensory pathway. J. Neurophysiol. 2004; 92:895–904. [PubMed: 15028739]

Liem KR Jr. Tremml G, Jessell TM. A role for the roof plate and its resident TGFβ-related proteins in neuronal patterning in the dorsal spinal cord. Cell. 1997; 91:127–138. [PubMed: 9335341]

Liu Y, Abdel Samad O, Zhang L, Duan B, Tong Q, Lopes C, Ji RR, Lowell BB, Ma Q. VGLUT2-dependent glutamate release from nociceptors is required to sense pain and suppress itch. Neuron. 2010; 68:543–556. [PubMed: 21040853]

Lizarraga I, Chambers JP, Johnson CB. Developmental changes in threshold, conduction velocity, and depressive action of lignocaine on dorsal root potentials from neonatal rats are associated with maturation of myelination. Can. J. Physiol. Pharmacol. 2007; 85:251–263. [PubMed: 17487267]

Maricich SM, Wellnitz SA, Nelson AM, Lesniak DR, Gerling GJ, Lumpkin EA, Zoghbi HY. Merkel cells are essential for light-touch responses. Science. 2009; 324:1580–1582. [PubMed: 19541997]

Maricich SM, Morrison KM, Mathes EL, Brewer BM. Rodents rely on Merkel cells for texture discrimination tasks. J. Neurosci. 2012; 32:3296–3300. [PubMed: 22399751]

McCrea DA. Spinal circuitry of sensorimotor control of locomotion. J. Physiol. 2001; 533:41–50. [PubMed: 11351011]

Mears SC, Frank E. Formation of specific monosynaptic connections between muscle spindle afferents and motoneurons in the mouse. J. Neurosci. 1997; 17:3128–3135. [PubMed: 9096147]

Mentis GZ, Siembab VC, Zerda R, Donovan MJ, Alvarez FJ. Primary afferent synapses on developing and adult Renshaw cells. J. Neurosci. 2006; 26:13297–13310. [PubMed: 17182780]

Mestre T, Lang AE. The grasp reflex: a symptom in need of treatment. Mov. Disord. 2010; 25:2479–2485. [PubMed: 20848621]

Monzee J, Lamarre Y, Smith AM. The effects of digital anesthesia on force control using a precision grip. J. Neurophysiol. 2003; 89:672–683. [PubMed: 12574445]

Moschovakis AK, Solodkin M, Burke RE. Anatomical and physiological study of interneurons in an oligosynaptic cutaneous reflex pathway in the cat hindlimb. Brain Res. 1992; 586:311–318. [PubMed: 1381652]

Müller T, Brohmann H, Pierani A, Heppenstall PA, Lewin GR, Jessell TM, Birchmeier C. The homeodomain factor lbx1 distinguishes two major programs of neuronal differentiation in the dorsal spinal cord. Neuron. 2002; 34:551–562. [PubMed: 12062039]

Napier JR. The prehensile movements of the human hand. J. Bone Joint Surg. Br. 1956; 38-B:902–913. [PubMed: 13376678]

Oliveira AL, Hydling F, Olsson E, Shi T, Edwards RH, Fujiyama F, Kaneko T, Hokfelt T, Cullheim S, Meister B. Cellular localization of three vesicular glutamate transporter mRNAs and proteins in rat spinal cord and dorsal root ganglia. Synapse. 2003; 50:117–129. [PubMed: 12923814]

Paulson G, Gottlieb G. Development reflexes: the reappearance of foetal and neonatal reflexes in aged patients. Brain. 1968; 91:37–52. [PubMed: 5643282]

Pearson KG, Acharya H, Fouad K. A new electrode configuration for recording electromyographic activity in behaving mice. J. Neurosci. Methods. 2005; 148:36–42. [PubMed: 15908013]

Pecho-Vrieseling E, Sigrist M, Yoshida Y, Jessell TM, Arber S. Specificity of sensory-motor connections encoded by Sema3e-Plxnd1 recognition. Nature. 2009; 459:842–846. [PubMed: 19421194]

Peyronnard JM, Charron L. Motor and sensory neurons of the rat sural nerve: a horseradish peroxidase study. Muscle Nerve. 1982; 5:654–660. [PubMed: 7155177]

Pietri T, Eder O, Blanche M, Thiery JP, Dufour S. The human tissue plasminogen activator-Cre mouse: a new tool for targeting specifically neural crest cells and their derivatives in vivo. Dev. Biol. 2003; 259:176–187. [PubMed: 12812797]

Pollack SL. The grasp response in the neonate; its characteristics and interaction with the tonic neck reflex. Arch. Neurol. 1960; 3:574–581. [PubMed: 13736833]

Quevedo J, Stecina K, Gosgnach S, McCrea DA. Stumbling corrective reaction during fictive locomotion in the cat. J.Neurophysiol. 2005; 94:2045–2052. [PubMed: 15917325]

Riddle CN, Baker SN. Convergence of pyramidal and medial brain stem descending pathways onto macaque cervical spinal interneurons. J.Neurophysiol. 2010; 103:2821–2832. [PubMed: 20457863]

Rogoz K, Lagerström MC, Dufour S, Kullander K. VGLUT2-dependent glutamatergic transmission in primary afferents is required for intact nociception in both acute and persistent pain modalities. Pain. 2012; 153:1525–1536. [PubMed: 22633683]

Rushworth G, Denny-Brown D. The two components of the grasp reflex after ablation of frontal cortex in monkeys. J. Neurol. Neurosurg. Psychiatry. 1959; 22:91–98. [PubMed: 13655096]

Scherrer G, Low SA, Wang X, Zhang J, Yamanaka H, Urban R, Solorzano C, Harper B, Hnasko TS, Edwards RH, Basbaum AI. VGLUT2 expression in primary afferent neurons is essential for normal acute pain and injury-induced heat hypersensitivity. Proc. Natl. Acad. Sci. USA. 2010; 107:22296–22301. [PubMed: 21135246]

Schieber MH. Dissociating motor cortex from the motor. J. Physiol. 2011; 589:5613–5624. [PubMed: 22005673]

Stepien AE, Tripodi M, Arber S. Monosynaptic rabies virus reveals premotor network organization and synaptic specificity of cholinergic partition cells. Neuron. 2010; 68:456–472. [PubMed: 21040847]

Sürmeli G, Akay T, Ippolito GC, Tucker PW, Jessell TM. Patterns of spinal sensory-motor connectivity prescribed by a dorsoventral positional template. Cell. 2011; 147:653–665. [PubMed: 22036571]

Takei T, Seki K. Spinal interneurons facilitate coactivation of hand muscles during a precision grip task in monkeys. J. Neurosci. 2010; 30:17041–17050. [PubMed: 21159974]

Todd AJ. Neuronal circuitry for pain processing in the dorsal horn. Nat. Rev. Neurosci. 2010; 11:823–836. [PubMed: 21068766]

Todd AJ, Hughes DI, Polgar E, Nagy GG, Mackie M, Ottersen OP, Maxwell DJ. The expression of vesicular glutamate transporters VGLUT1 and VGLUT2 in neurochemically defined axonal populations in the rat spinal cord with emphasis on the dorsal horn. Eur. J. Neurosci. 2003; 17:13–27. [PubMed: 12534965]

Tripodi M, Stepien AE, Arber S. Motor antagonism exposed by spatial segregation and timing of neurogenesis. Nature. 2011; 479:61–66. [PubMed: 22012263]

Vrieseling E, Arber S. Target-induced transcriptional control of dendritic patterning and connectivity in motor neurons by the ETS gene Pea3. Cell. 2006; 127:1439–1452. [PubMed: 17190606]

Walshe F, Hunt J. Further observations upon grasping movements and reflex tonic grasping. Brain. 1936; 59:315–322.

Wang Z, Li L, Goulding M, Frank E. Early postnatal development of reciprocal Ia inhibition in the murine spinal cord. J. Neurophysiol. 2008; 100:185–196. [PubMed: 18463181]

Watson, C.; Paxinos, G.; Kayalioglu, G. The Spinal Cord: A Christopher and Dana Reeve Foundation Text and Atlas. Acadamic Press; London: 2008.

Witney AG, Wing A, Thonnard JL, Smith AM. The cutaneous contribution to adaptive precision grip. Trends Neurosci. 2004; 27:637–643. [PubMed: 15374677]

Young RW. Evolution of the human hand: the role of throwing and clubbing. J. Anat. 2003; 202:165–174. [PubMed: 12587931]

Highlights

- Spinal dI3 interneurons are glutamatergic and project to motoneurons
- dI3 interneurons receive direct primary afferent inputs from cutaneous afferents
- Silencing the output of dI3 interneurons disrupts a disynaptic cutaneous reflex
- dI3 interneurons mediate cutaneous control of paw grasp

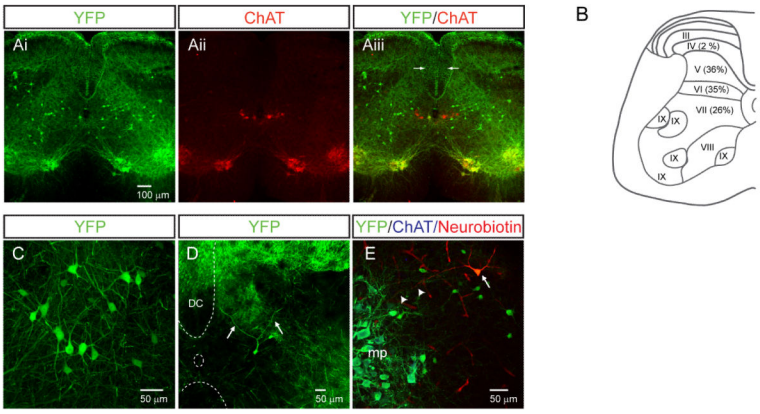

Figure 1. dI3 INs are multipolar spinal interneurons located in the deep dorsal horn and the intermediate laminae of the spinal cord

(A) Transverse distribution of YFP and ChAT labeled spinal neurons in a lumbar spinal cord section. Note the expected expression in dorsal root ganglion neurons as seen by fluorescence in axons in the dorsal columns (arrows) and dorsal horns.

(B) Laminar distribution of dI3 INs based upon cell counts from ten transverse L4/L5 sections. Laminae divisions based upon Watson et al. (2008).

(C) dI3 INs are multipolar neurons with multiple dendrites. The somata of dI3 INs were of intermediate size (17.5 ± 3.7 µm, n = 95) and multipolar in shape with, on average, 3.9 ± 3.7 (n = 95) primary dendritic trees.

(D) dI3 IN with dendrites (arrows) extending into lamina IV-VI of the dorsal horn. Dorsal column (DC), central canal (oval) and ventral white matter are delineated by dashed curves.

(E) Neurobiotin-filled dI3 IN (arrow) with dendritic process (arrowheads) extended towards motor pools (mp).

All images from *Isl1*-YFP mice. See also Figure S1.

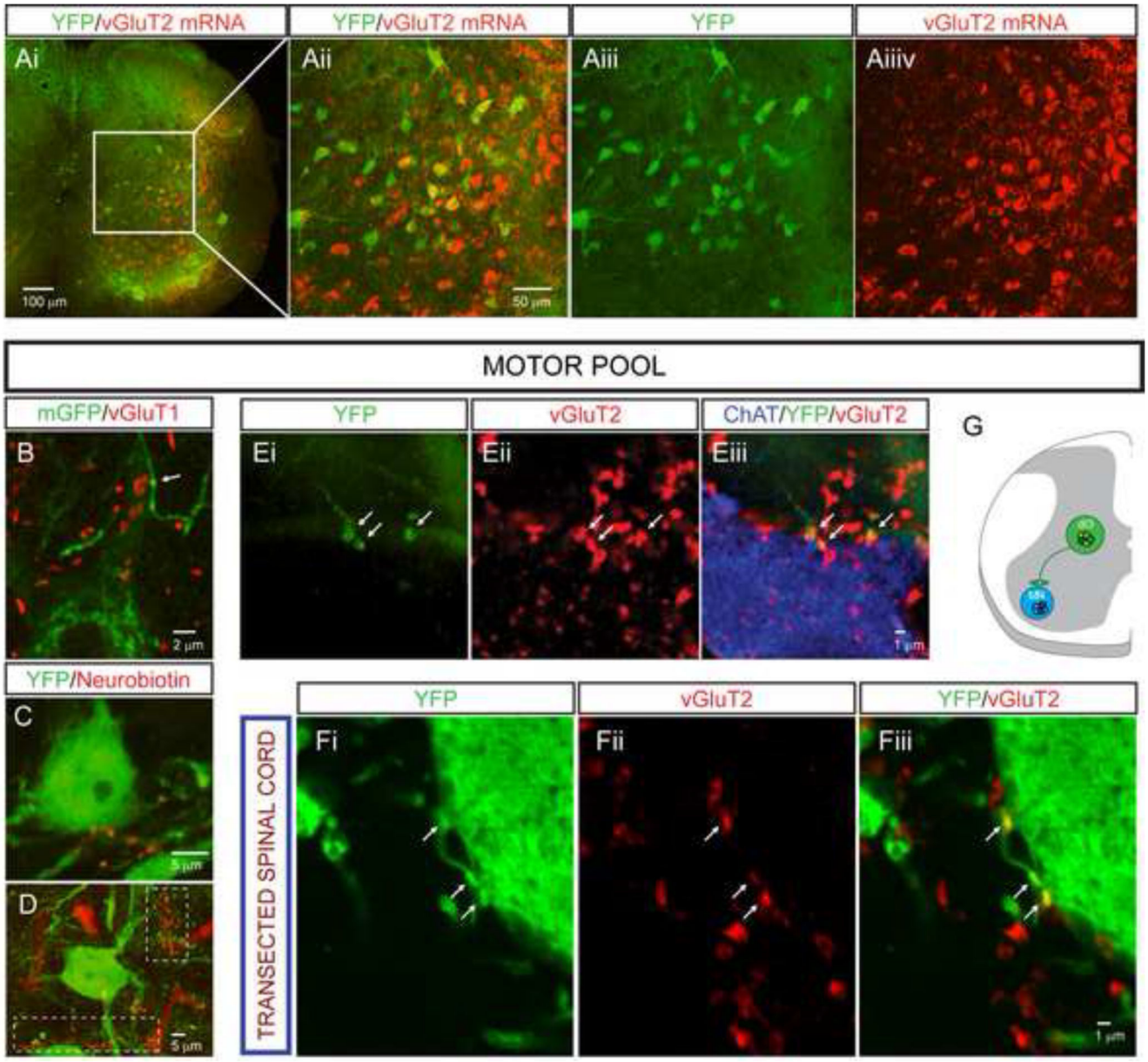

Figure 2. dI3 INs are excitatory premotor interneurons

(A) In-situ hybridization for vGluT2 mRNA colocalizes with YFP$^+$ interneurons in lamina V-VII. Quantitative analysis was restricted to laminae V-VII to avoid sampling YFP$^+$ somatic motoneurons in laminae IX, and revealed that 118/139 YFP+ neurons clearly expressed vGluT2.

(B) YFP$^+$ motoneuron in lamina IX with YFP$^+$ bouton-like structures (arrow) from putative dI3 INs in a spinal cord of a *Isl1*$^{+/Cre}$; *Thy1*.lox-stop-lox.mGFP mouse. vGluT1 is labeled in red, demonstrating that these processes are not from primary afferents.

(C and D) YFP$^+$ motoneurons in lamina IX motor pool with bouton-like processes from neurobiotin-labeled dI3 IN. Thick red processes are blood vessels. White dashed boxes highlight clusters of filled boutons.

(E) $YFP^+/vGluT2^+$ boutons (arrows) apposed on motoneuron (labeled with ChAT).
(F) $YFP^+/vGluT2^+$ boutons (arrows) apposed to motoneuron processes in chronically transected spinal cord.
(G) Diagram representing dI3 INs as last-order, excitatory interneurons.
Unless otherwise noted, all images from *Isl1*-YFP mice. See also Figure S2.

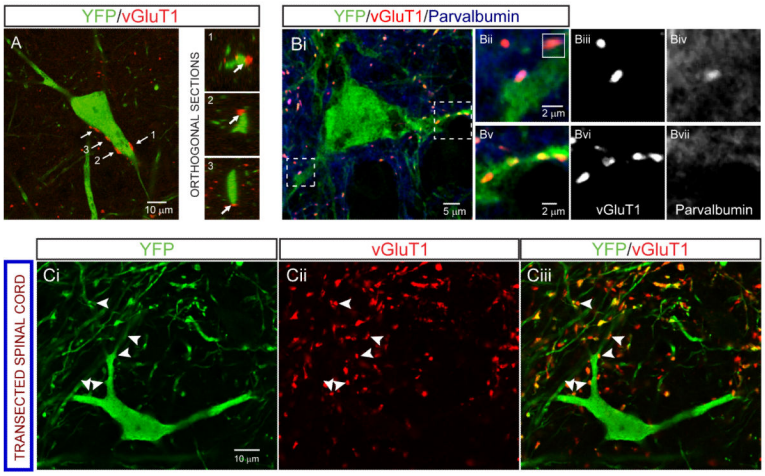

Figure 3. Anatomical evidence that primary afferents project to dI3 INs

(A) Left: YFP^{+} dI3 IN with vGluT1^{+} boutons apposed (labeled by arrows). Right: Orthogonal sections confirming apposition of boutons labeled 1-3.

(B) vGluT1^{+} boutons that are PV^{+} and PV^{null} on a YFP^{+} dI3 IN from a P7 spinal cord. Boutons in dashed boxes are magnified in Bii-Bvii. Inset in 3Bii depicts orthogonal sections of the PV^{+}/YFP^{+} bouton in the Y-Z plane.

(C) vGluT1^{+} boutons (arrowheads) on YFP^{+} dI3 IN from chronically transected spinal cord confirm that they do not originate from supraspinal descending inputs.

All images from *Isl1*-YFP mice.

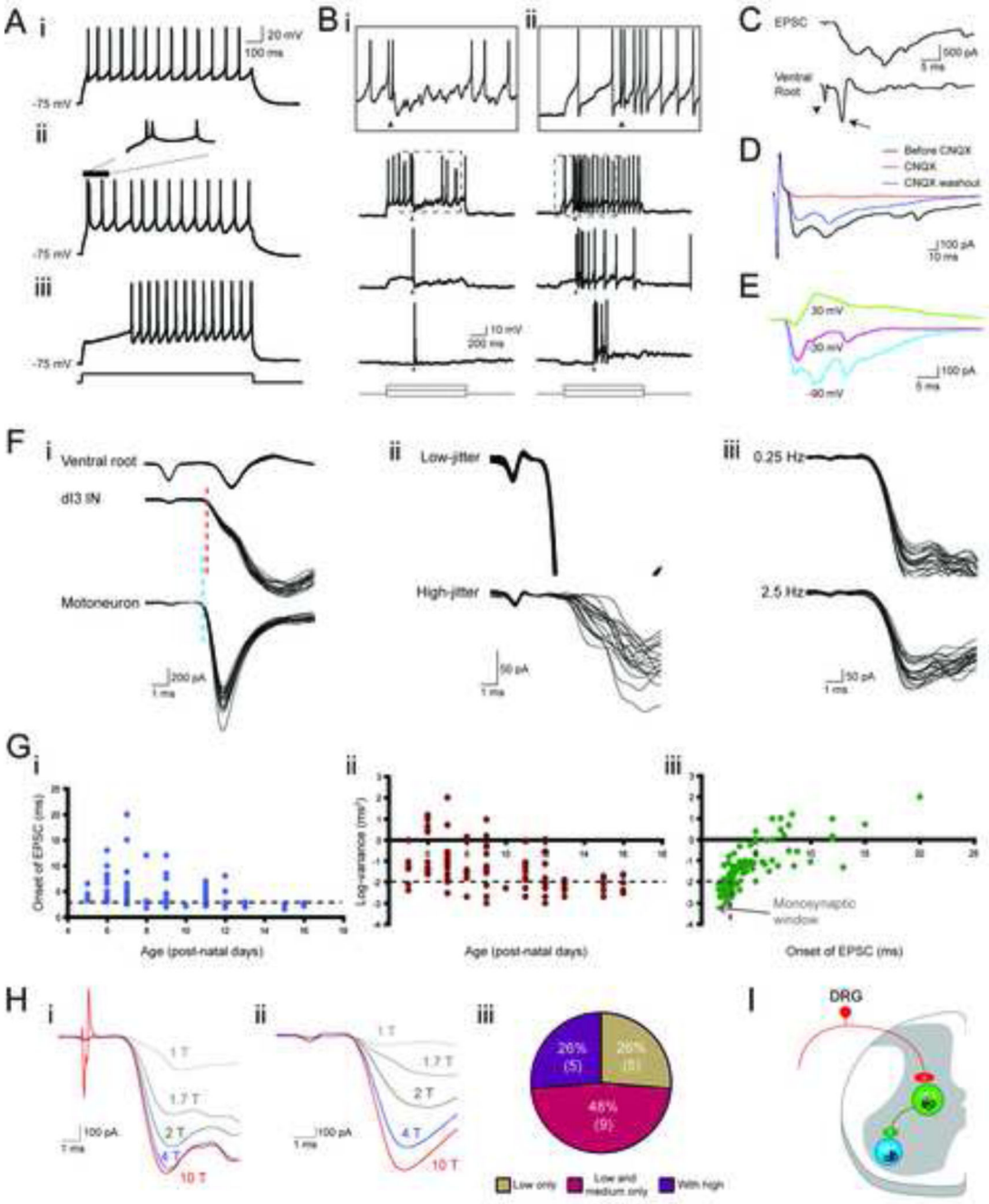

Figure 4. Response of dI3 INs to sensory afferent stimulation

(A) Three types of firing behaviors. i. Tonic firing. ii. Initial bursting. iii. Delayed firing. (B) Current-clamp recording of two dI3 INs showing response to DR stimulation (20 μA, just under 3 × T, 250 μs) during current steps of three different magnitudes. i. Cell responding with an action potential followed by a prolonged hyperpolarization. ii. Cell responding with a prolonged depolarization. Arrowheads mark the time of stimulation. Top row is a scaled version of area marked by dashed box in second row.

(C) Voltage-clamp recording of L5 dI3 IN depicting an EPSC in response to DR stimulation (20 μA, just under 3 × T, 250 μs) with accompanying extracellular ventral root (L5) recording. Arrowhead marks the stimulation artifact while the arrow marks the monosynaptic ventral root response.
(D) EPSCs in response to DR stimulation (20 μA, just under 3 × T) reversibly blocked by CNQX.
(E) drEPSCs at different holding potentials showing reversal of EPSC at depolarized potential.
(F) Demonstration of monosynaptic nature of sensory input. i. Onset of drEPSC (15 μA, 3 × T) in dI3 IN as compared to onset of monosynaptic EPSC in a motoneuron from the same preparation. These two cells were recorded separately. The ventral root recording was concomitant with the motoneuron recording. The timing of the ventral root response during dI3 IN recording was the same. Blue dashed line marks the onset of the motoneuron EPSC. Red dashed line marks the onset of the dI3 IN EPSC. The difference was below 0.2 ms. ii. Top: drEPSCs (15 μA, 3 × T) in dI3 IN with low jitter (0.002 ms^2). Jitter calculated on 20 responses. Bottom: drEPSCs (20 μA, 4 × T) in dI3 IN with high-jitter (0.47 ms^2). iii. Low-latency, low-jitter drEPSCs in dI3 IN with no failures in response to 0.25 and 2.5 Hz stimulation frequency (n = 3), confirming these are monosynaptic responses.
(G) Shift towards monosynaptic sensory inputs with age. Relation between i. Onset of drEPSC in dI3 INs and age, ii.Variance of drEPSC onset and age, and iii.Variance of drEPSC onset and onset of drEPSC.
(H) Response to different strengths of DR stimulation. i. dI3 IN with increases in drEPSC magnitude with shift from low to medium strength but not to high threshold dorsal root stimulation. ii. dI3 IN with increases in drEPSC magnitude with shift from low to medium to high threshold dorsal root stimulation. T refers to the threshold at which a monosynaptic ventral root reflex was elicited. iii. Distribution of sets of responses in dI3 INs to DR stimulation (single 250 μs pulses). Low threshold fibers were considered to be recruited by stimulation between 1-2 × T, medium threshold fibers were recruited by 2-5 × T, and high threshold fibers were recruited by stimulation above 5 × T. T is the earliest stimulation strength at which a monosynaptic ventral root reflex was elicited in ventral roots. Number of cells in parentheses.
(I) Diagram representing dI3 INs as part of a disynaptic pathway between sensory input and motoneurons.
See also Figure S3.

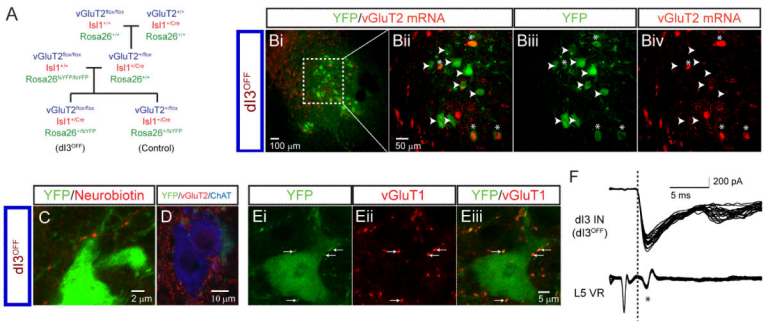

Figure 5. Loss of vGluT2 expression in dI3^{OFF} mice

(A) Breeding strategy to generate silencing of the output of dI3 INs (dI3^{OFF}) by conditionally knocking out vGluT2. fsYFP refers to lox-stop-lox.YFP. Only the genotypes that were used are shown.

(B) Fluorescent in-situ hybridization shows reduced presence of vGluT2 mRNA to 28% of YFP^{+} dI3 INs, (n = 92 out of 330 neurons from 2 mice) in dI3^{OFF} animals. Asterisks denote dI3 INs with presence of vGluT2 mRNA, arrowheads denote dI3 INs with absence of vGluT2 mRNA.

(C) Following neurobiotin injection in a dI3 IN from a dI3^{OFF} animal, bouton-like appositions are present on a putative YFP^{+} motoneuron in lamina IX.

(D) Loss of vGluT2^{+}/YFP^{+} boutons on ChAT^{+} motoneuron.

(E) vGluT1^{+} inputs to YFP^{+} dI3 INs are still present in dI3^{OFF} mice (8/9 dI3 INs).

(F) Ventral-root reflex and monosynaptic dorsal root-evoked EPSCs in dI3 INs are present in dI3^{OFF} mice (8 out of 10 dI3 INs showed dorsal-root evoked EPSCs; 4/10 dI3 INs met strict short–latency, low jitter thresholds as above). Interestingly, these mice became pruritic (Figure S4B), as might be expected from loss of vGluT2 from high threshold afferents (Lagerström et al., 2010; Liu et al., 2010).

All images from lumbar spinal cord of P13-16 dI3^{OFF} mice. See also Figure S4.

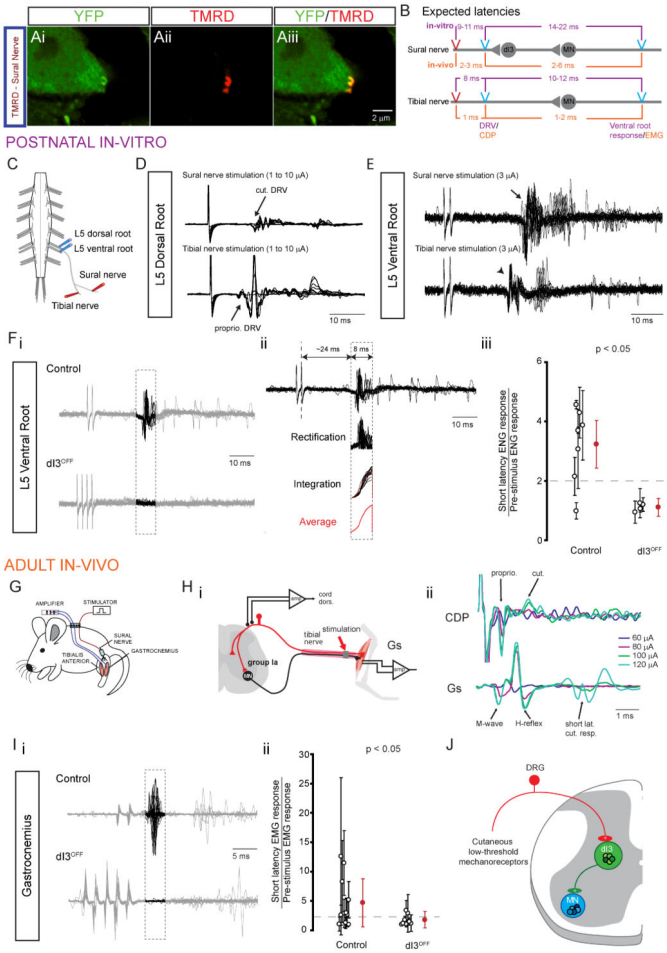

Figure 6. Conditional silencing of the output of dI3 INs abolishes short latency response to cutaneous nerve stimulation

(A) Tetramethylrhodamine (TMRD)$^{+}$ boutons on YFP^{+} dI3 IN in a *Isl1*-YFP spinal cord three days after TMRD labelling of sural nerve, a predominantly cutaneous nerve (Peyronnard and Charron, 1982).

(B) Schematic describing the estimated latencies of monosynaptic and disynaptic ventral root reflexes in response to tibial and sural nerves, respectively. Estimates were calculated for experiments with postnatal isolated spinal-cord preparation with sural nerve left in continuity and for adult in-vivo recordings. They were based upon observed latencies between stimulation, DR volley or CDP, and ventral root reflexes or EMG recordings.

(C) Scheme of isolated spinal-cord preparation with sural nerve left in continuity. Stimulating electrodes were placed on the sural nerve and the tibial nerve distal to the sural nerve branchpoint. Recording electrodes were placed on the ipsilateral L5 dorsal and ventral roots.

(D) L5 dorsal root potentials in response to sural nerve or tibial nerve stimulations. In this example, the earliest DR volley to sural nerve and tibial nerve stimulations were seen at 3 and 2 µA, respectively.

(E) 20 traces of L5 ventral root reflexes elicited by two 250 µs shocks (500 Hz) applied to the sural nerve and the tibial nerve. Note the low-jitter monosynaptic reflex in response to

tibial nerve stimulation (arrowhead) versus the high-jitter short-latency oligosynaptic reflex in response to sural nerve stimulation (arrow).

(F) i. Recordings of L5 ventral root ENGs to multiple stimulation pulses applied to the sural nerve. Putative disynaptic reflex responses are highlighted in dashed box. ii. Methodology for quantification of short-latency response in 8-ms time window, 14 ms from low-threshold, earliest L5 DR volley from sural nerve stimulation (not shown). iii. Summary of short-latency L5 ventral root ENG reflex response to sural nerve stimulation. Data point shows the ratio of the time-integrated ENG response to sural nerve stimulation in the short-latency ENG time-window over the time-integrated ENG response in a randomly selected 8-ms time-window prior to the application of the stimulus trains. Clear circles represent each isolated spinal cord, filled circles represent group average. Error bars represent SD. Dashed line represents reflex threshold of 2.

(G) Scheme of EMG recordings of chronically implanted electrodes into Gs and TA muscles of control and $dI3^{OFF}$ mice.

(H) Recordings of cord dorsum potentials (CDPs) in response to tibial nerve stimulation. i. Recording set up. ii. (top) CDP showing activation of proprioceptive and cutaneous potentials with increasing current stimulation, (bottom) corresponding EMG recording of Gs.

(I) i. Recordings of Gs EMG to multiple stimulation pulses applied to the sural nerve. Putative disynaptic reflex responses are highlighted in dashed box. ii. Summary of short-latency synaptic EMG response reflex response measured in a 4-ms time-window, 4 ms after the onset of the last stimulation pulse to sural nerve stimulation. Data point shows the ratio of the time-integrated EMG response to sural nerve stimulation in the short-latency EMG time-window over the time-integrated EMG response in a randomly selected 4-ms time-window prior to the application of the stimulus trains. Clear circles represent each animal, filled circles represent group average. Error bars represent SD. Dashed line represents reflex threshold of 2.

(J) Diagram representing dI3 INs as part of a disynaptic pathway between low threshold mechanoreceptors from the skin and motoneurons.

See also Figure S5.

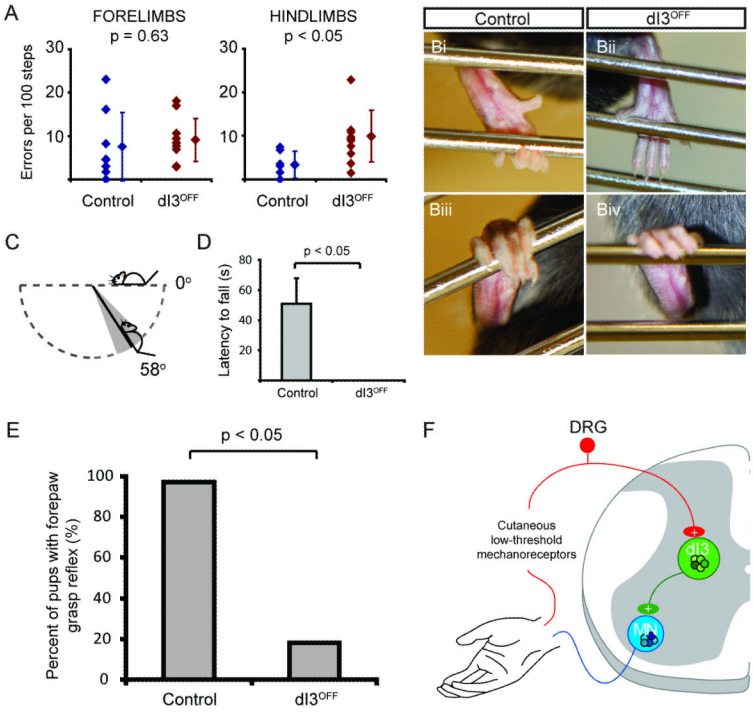

Figure 7. Reduced performance in several motor tasks involving cutaneous afferents from the paw, including loss of functional grip in dI3^{OFF} mice

(A) During ladder walking with rung spacing of 2 cm, forelimb errors are similar in controls and mutants, whereas the mutants have more hindlimb errors than controls. Error bars represent SD.

(B) Comparison of hindlimb grip of a metal bar between control and dI3^{OFF} mice.

(C) In the wire hang test, control animals grip onto the cage top, while upside down, for close to one minute whereas the dI3^{OFF} mice are unable to hang onto the cage top while inverted. Diagram depicting minimal angle from horizontal axis at which dI3^{OFF} mice are unable to hang onto the cage top. The grey cone represents the pooled SD.

(D) Performance of control and dI3^{OFF} mice during the wire hang test. The maximal duration of the test was one minute. Every control animals would hang on for periods longer than a minute in at least one of three trials. Similar results were observed when mice were tested a second time one or two days later. Error bars represent SD. See also Movies S1 and S2.

(E) Forepaw grasp reflex in control and dI3^{OFF}postnatal (P1-P7) mice. Chi-square test indicated.

(F) Diagram representing dI3 INs as part of a disynaptic pathway between low threshold mechanoreceptors from the skin and motoneurons involved with regulating grip strength.